small
NANO MICRO
www.small-journal.com

Out-of-Plane 3D-Printed Microfibers Improve the Shear Properties of Hydrogel Composites

Mylène de Ruijter, Andrei Hrynevich, Jodie N. Haigh, Gernot Hochleitner, Miguel Castilho, Jürgen Groll, Jos Malda, and Paul D. Dalton**

One challenge in biofabrication is to fabricate a matrix that is soft enough to elicit optimal cell behavior while possessing the strength required to withstand the mechanical load that the matrix is subjected to once implanted in the body. Here, melt electrowriting (MEW) is used to direct-write poly(ε-caprolactone) fibers "out-of-plane" by design. These out-of-plane fibers are specifically intended to stabilize an existing structure and subsequently improve the shear modulus of hydrogel–fiber composites. The stabilizing fibers (diameter = 13.3 ± 0.3 µm) are sinusoidally direct-written over an existing MEW wall-like structure (330 µm height). The printed constructs are embedded in different hydrogels (5, 10, and 15 wt% polyacrylamide; 65% poly(2-hydroxyethyl methacrylate) (pHEMA)) and a frequency sweep test (0.05–500 rad s^{-1}, 0.01% strain, $n = 5$) is performed to measure the complex shear modulus. For the rheological measurements, stabilizing fibers are deposited with a radial-architecture prior to embedding to correspond to the direction of the stabilizing fibers with the loading of the rheometer. Stabilizing fibers increase the complex shear modulus irrespective of the percentage of gel or crosslinking density. The capacity of MEW to produce well-defined out-of-plane fibers and the ability to increase the shear properties of fiber-reinforced hydrogel composites are highlighted.

M. de Ruijter, Dr. M. Castilho, Prof. J. Malda
Department of Orthopedics
University Medical Center, Utrecht University
P.O. Box 85500, 3508 GA Utrecht, The Netherlands
E-mail: j.malda@umcutrecht.nl
A. Hrynevich, J. N. Haigh, G. Hochleitner,
Prof. J. Groll, Prof. P. D. Dalton
Department of Functional Materials in Medicine
and Dentistry and Bavarian Polymer Institute
University Hospital of Würzburg
Pleicherwall 2, 97070 Würzburg, Germany
E-mail: paul.dalton@fmz.uni-wuerzburg.de
Dr. M. Castilho
Department of Biomedical Engineering
Eindhoven University of Technology
P. O. Box 513, 5600 MB Eindhoven, The Netherlands
Prof. J. Malda
Department of Equine Sciences
Faculty of Veterinary Sciences
Utrecht University
Yalelaan 112, 3584 CM Utrecht, The Netherlands
The ORCID identification number(s) for the author(s) of this article can be found under https://doi.org/10.1002/smll.201702773.

DOI: 10.1002/smll.201702773

Melt electrowriting (MEW) is an additive manufacturing technique that direct-writes ultrafine fibers onto a surface using molten fluid columns that are stabilized with an applied voltage.[1–3] The process is different to polymer melt,[4] hydrogel,[5] and colloidal ink[6,7] extrusion through nozzles which all operate with direct-contact deposition for each layer. In this study, the electrified molten jet is periodically written back and forth across a wall-like structure with remarkable consistency, with minimal variation in structural dimensions. When embedded within a hydrogel, these "out-of-plane fibers" distinctly increase the shear modulus of the composite, even though they partake in a small fraction of the total composite volume.

Previously MEW has been used for "in-plane" printing, meaning that the fiber is aligned along a single plane for cartesian coordinates,[1] or a single curvature for rotating collectors.[8] The technique is capable of producing micrometer-scale diameter fibers, ranging from 45 µm[1] to as small as 820 nm.[9] In addition, MEW results in a narrow fiber diameter distribution (3–5% coefficient of variation), emphasizing the reproducibility of this technique.[10] The accurate and reproducible fiber deposition is a crucial characteristic for the use of such a technology in biomedicine, filtration, and energy applications.[11–15]

The mechanical advantage of accurate control over fiber placement was shown in a recent study, where a weak hydrogel matrix was reinforced with either small-diameter MEW (2–7 vol%) fibers or with thicker (16 vol%) fused deposition modeling (FDM) fibers.[16] The MEW-reinforced constructs were able to recapitulate the compressive properties of native articular cartilage, whereas the FDM fibers-containing structures were significantly stiffer than the native tissue and failed at comparatively low deformations (less than 10% strain).[16] The implications for tissue engineering (TE) applications is that such fiber/hydrogel composites enable the use of a mechanically weak hydrogel for cell differentiation and matrix formation, while still providing a structural support required for high compressive loading conditions.[17]

Other methods to reinforce hydrogels include using random solution electrospun meshes,[18] interpenetrating polymer networks,[19] or the inclusion of carbon nanofiber tubes.[20] However, the restricted control over the fiber meshes architectures limits their reinforcing potential of soft hydrogels by

such meshes. MEW is distinct from these approaches as it allows for fiber placement control with highly organized architecture that synergistically reinforces hydrogels in compression.[16,21] Control over design in reinforcing techniques is also shown with FDM and extrusion based bioprinting for poly(ε-caprolactone) (PCL)-based and hydrogel-based reinforcement, respectively.[16,22] Nonetheless, the accuracy and fiber resolution limits of such extrusion-based fabrication methods hinder the reinforcing potential. Extrusion direct writing is also associated with a high volume fraction of reinforcing materials that can result in stress shielding compromising a favorable mechanoregulated environment for the cells to differentiate and excrete extracellular matrix.[23] The reinforcement with "woodpile" MEW fibers showed promising results with regard to the resistance to compressing forces,[16] however, it did not address the interplay of compressive, shear, and tensile stresses that tissues in the human body are subjected to. Therefore, to generate hydrogel-based constructs for the replacement of damaged tissues, additional scaffold design elements for fiber-reinforcement are required.

The effect of introducing a fiber that crosses through a layered MEW structure (described herein as a "wall") is quantitatively explored, using out-of-plane deposition. Such crossing fibers (described herein as "stabilizing fibers") are fabricated to stabilize the wall under shear forces when embedded in a hydrogel. To accurately evaluate the shear properties, the fiber/hydrogel composite samples were designed for analysis with a rotational shear rheometer. An understanding of the basic requirements for improving the resistance to shear stresses is investigated prior to enable these elements to be combined into physiologically relevant fiber/matrix composites for TE applications. The unit structure for a stabilizing fiber is shown in **Figure 1**A and has a specific wavelength, amplitude, and fiber span. Scanning electron microscopy (SEM) revealed that the out-of-plane MEW fiber contains very defined and reproducible features (Figure 1B). This reproducibility was emphasized by the outcomes of the quantitative SEM analysis (Figure 1C) that revealed that the span of the ascending (114.02 ± 5.98 µm) and descending fiber (151.24 ± 6.69 µm) was significantly different ($p < 0.05$) from each other, and increased with an increase of the wall height. Unlike

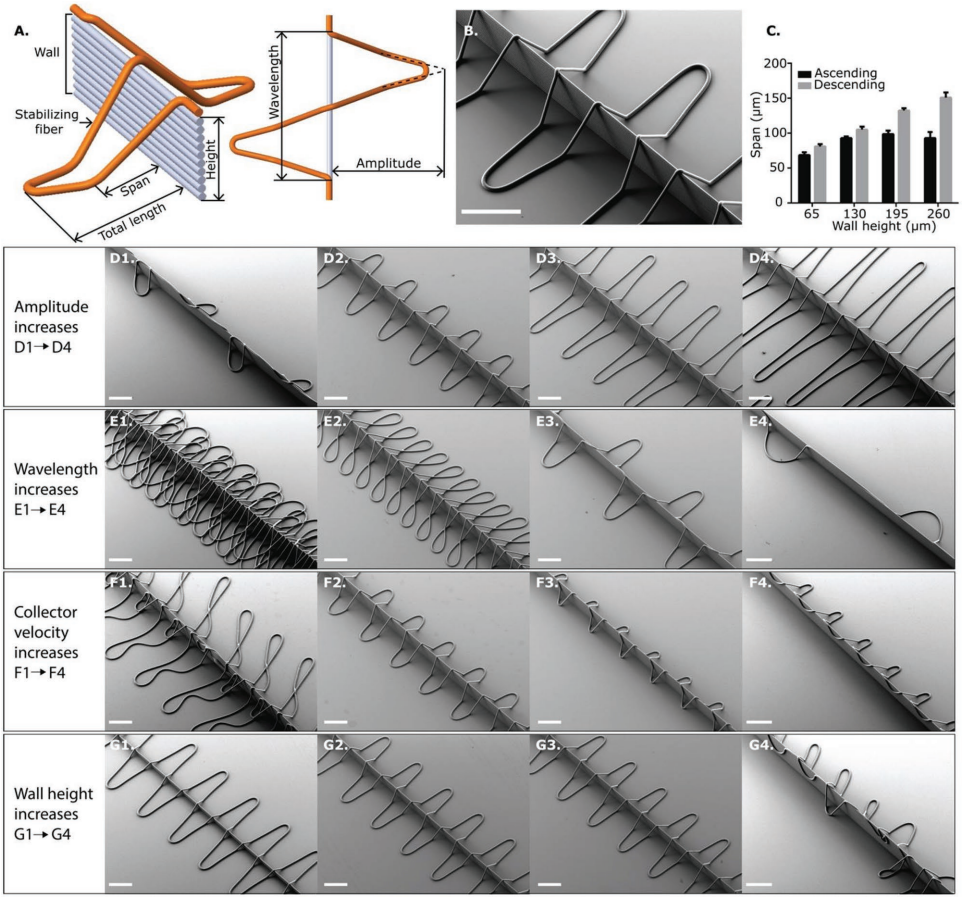

Figure 1. Fabrication of stabilizing fibers. A) Illustration and nomenclature of stabilizing fibers that were deposited out-of-plane. B) Stabilizing fibers crossing the wall with programmed amplitude = 500 µm, wavelength = 400 µm, collector velocity = 400 mm min^{-1}. Scale bar = 100 µm. C) Effect of the height of the wall on the span of the ascending and descending fiber. D) Effect of amplitude on stabilizing fiber fabrication. Wavelength and collector velocity similar as (B). E) Effect of wavelength on the morphology of the stabilizing fibers. Amplitude and collector velocity similar as (B). F) Effect of collector velocity on stabilizing fiber fabrication. Amplitude and wavelength similar to (B). G) Effect of height on stabilizing fiber fabrication with parameters as in (B). Scale bar = 200 µm.

for extrusion direct-writing, for MEW the high voltage applied between the nozzle and collector affects accurate fiber deposition, particularly when existing structures are present on the collector. This includes previously deposited MEW fibers (i.e., the wall), which can consequently attract (or repulse) the subsequently deposited layer, depending on the polymer composition.[1,10,24,25]

The fiber diameter for both the wall and stabilizing fibers was 13.3 ± 0.3 μm. Nevertheless, the collector movement amplitude and wavelength, the collector velocity, and height of the wall, all affect morphology of the stabilizing fibers. Optimal stabilizing fiber morphology included fibers that cross the wall in a straight manner (i.e., without being deflected or overlapping) and were created with a collector movement amplitude of 500 μm, wavelength of 400 μm, collector velocity of 400 mm min^{-1}, at a wall height of 20 layers (265 μm). When the amplitude was decreased to the lower limit of 200 μm, stabilizing fibers only minimally spanned the wall to the collector, and often adhered to the side of the wall (Figure 1D). When increasing this amplitude to 1000 μm, the span remained constant while the length of the fiber that adheres to the collector increased (Figure S1A, Supporting Information). Fibers that were deposited with a small wavelength resulted in stabilizing fibers that intersected already deposited stabilizing fibers (Figure 1E). Increasing the wavelength decreased both the span and the total length of the fiber (Figure S1B, Supporting Information).

It is important to note that the electrified molten jet for MEW deposits onto the collector in a similar manner to noncharged viscoelastic fluids.[10,26–28] To deposit linear fibers, the collector speed must at least match the speed of the electrified jet. The speed at which the electrified jet and collector match has been previously termed the critical translation speed (CTS).[1,10,29] When depositing stabilizing fibers with a velocity below the CTS, an irregular pattern was clearly observed and the fibers buckled and collapsed onto the wall (Figure 1F). An increase in collector velocity did not affect the span of the stabilizing fiber (Figure S1D, Supporting Information), however, it did decrease the total length of the stabilizing fiber, due to writing with a viscoelastic fluid. A clear increase in span was observed when the wall-height was increased (Figure 1G,C). However, an upper limit of 20 layers (265 μm) was found with the selected parameters, since stabilizing fibers started to adhere to the wall at a wall-height of 25 layers (330 μm).

Overall, these data show the influence of the instrument parameters on fiber morphology. For the first time, the morphology of fibers fabricated with MEW includes an intentionally introduced out-of-plane component. By tailoring the machine parameters, fiber morphology could be altered resulting in highly reproducible structures (Figure 1B) that could potentially be used to reinforce hydrogels.

While there are potential applications of spanning microstructures within electronics,[30–32] our interest in such stabilizing fibers was to enhance the shear properties of fiber/hydrogel composites for use in medical and TE applications. Therefore, MEW scaffolds were fabricated in a radial configuration so that the stabilizing fibers were in the same direction as the applied load of the rotational shear rheometer (SF1; **Figure 2**A), and walls only (Figure 2B) were used as the control. A single fiber grid layer was first direct written under all samples to assist in fiber adhesion and handling during hydrogel embedding (Figure 2C).

In order to determine the effect of fiber architecture on the resistance to shear, multiple designs, with extra stabilizing fibers incorporated within the structure, were also fabricated (Figure 2D,E). For these additional groups, the stabilizing fibers were integrated within the top of the wall by alternating the stabilizing fibers with the fibers being placed upon the wall (Figure 2F). One variant had four stabilizing fibers in total, with half of them out-of-phase with each other (SF2; Figure 2D) while the other one had all four stabilizing fibers in phase (SF3; Figure 2E). To analyze the effect of the stabilizing fibers on the shear modulus of PCL/hydrogel composites, these 3D MEW structures were embedded in different concentrations of polyacrylamide with a range of crosslinking densities, as well as in poly(2-hydroxyethyl methacrylate) (pHEMA). All fiber/hydrogel constructs had a relatively low PCL component of only 0.24–0.29 vol% (i.e., a hydrogel content between 99.71 and 99.76 vol%) (Figure 2B–F). The inclusion of stabilizing fibers within the various hydrogels did increase the shear modulus for all different geometries (walls only, SF1, SF2, and SF3; see **Figure 3**A), both in the pHEMA and in the relatively soft 5% polyacrylamide (Figure 3B,C). Remarkably, no significant differences were found between the variant groups geometries (SF1, SF2, and SF3) with additional fibers integrated into the structure—as long as there was a stabilizing fiber, the shear modulus of the composite increased to a similar level. To investigate the effect of hydrogel-concentration and crosslink-density of the hydrogel on the fiber reinforcement effect, stabilizing fibers were tested in 5%, 10%, and 15% polyacrylamide and with 0.2, 0.3, and 0.5% bis-acrylamide (Figure 3D–F). Although no correlation was found, the reinforcing effect of the stabilizing fibers was shown in all gels, irrespective of hydrogel-concentration or crosslink-density. A deeper understanding of this reinforcing effect for shear forces could be achieved using numerical methods to investigate the influence of out-of-plane fibers, including their morphology and more complex organizations, on the mechanical behavior and reinforcement mechanism of soft hydrogels. The use of continuum finite element methods, combined with experimental data, can provide a better understanding of the construct's mechanical response with different boundary conditions, e.g., confined compression, shear loading, or other boundary conditions that mimic a specific physiological application and eventually facilitate the reinforcing strategy design process. This in turn would provide reinforcement designs for MEW with even more efficiency and complexity.

In conclusion, this study shows the highly reproducible out-of-plane deposition of an electrically charged polymer melt, resulting in stabilizing fibers. Stabilizing structures, irrespective of the number and arrangement of fibers (in phase or out of phase), increased the shear modulus in both weak and strong hydrogels, with different crosslinking densities and different hydrogel concentrations. The ability to fabricate highly reproducible MEW structures that include an out-of-plane component and the capacity to increase the shear response of hydrogel/fiber composites, while maintaining a soft hydrogel, are key outcomes of this study.

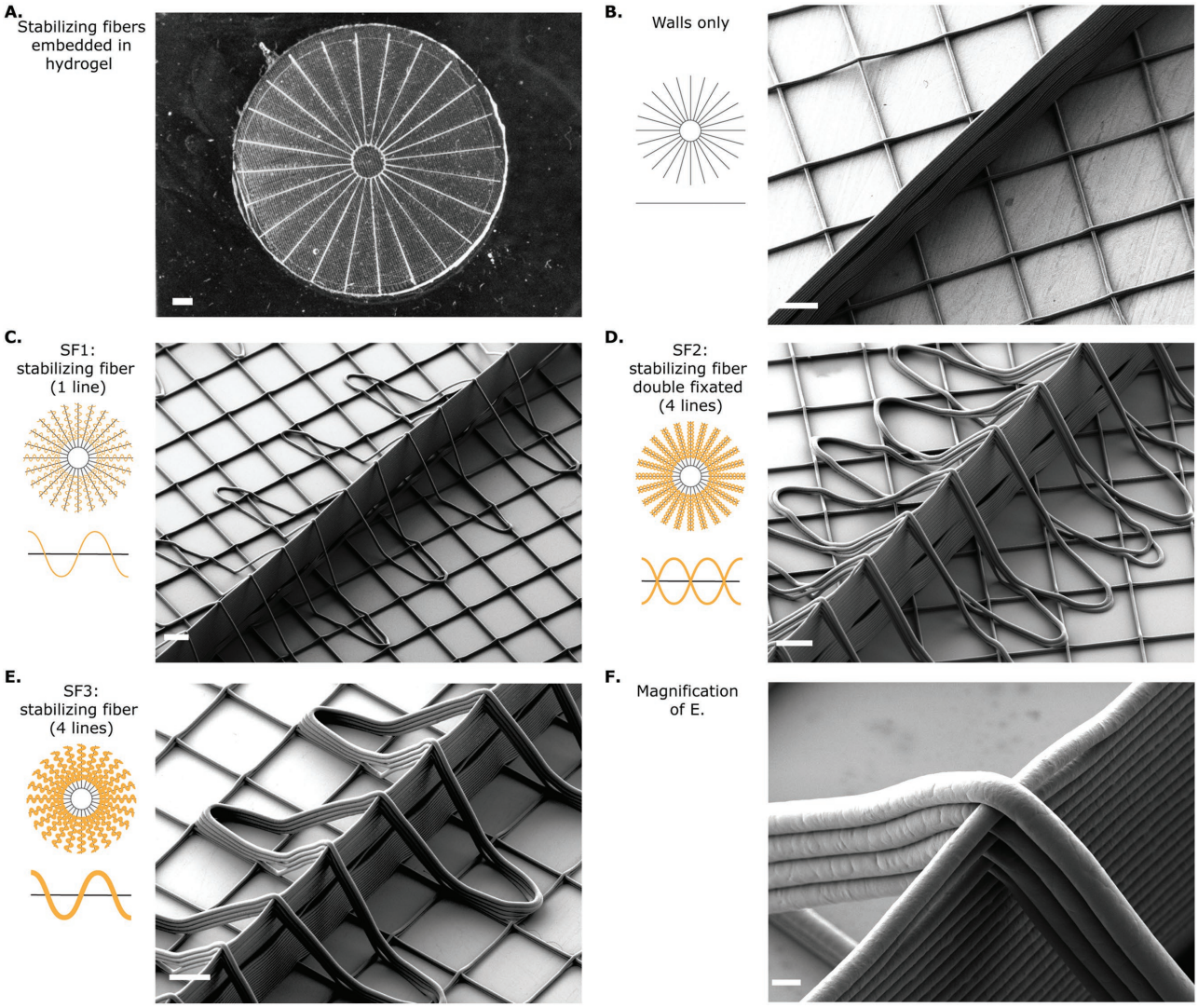

Figure 2. Different variants of stabilizing fibers produced in a radial manner for shear stress measurements. A) Overview image of a MEW PCL scaffold embedded in a model hydrogel. B) Control group, walls only, no stabilizing fibers. C) Stabilizing fibers, 1 line. D) Stabilizing fibers, 4 lines of which 2 out of phase. E) Stabilizing fibers, 4 lines, in-phase. F) Magnification of (E), where the stabilizing fibers cross the wall. Scale bar (A) = 1 mm, scale bar (B–E) = 100 µm, scale bar (F) = 10 µm.

Experimental Section

Materials: For all experiments PCL (PURASORB PC 12, Lot# 1412000249, 03/2015, Corbion Inc., Gorinchem, Netherlands) was used for MEW. The PCL was stored and retrieved using procedures previously outlined.[10] In order to erase previous thermal history before first use, the polymer was heated to 90 °C for 30 min, cooled down to room temperature, and heated up to 90 °C again. After this, each PCL sample was used for a maximum period of 100 h to avoid degradation of the polymer.

MEW Device: A custom-built MEW device that included high precision *x*–*y*–*z* linear axes (Aerotech Inc., Pittsburgh, USA) with a reported resolution of 1 µm was used. The opposed aluminum collector plate was grounded and moved in *X*- and *Y*-directions via PRO115-05MM-150-UF positioning stage while the nozzle was moved in the *Z*-direction via an ATS03005 stage. The axes were controlled via G-code, using A3200 Motion Composer (A3200, version 4.09.000.0126, Aerotech Inc., Pittsburgh, USA). A precision pressure control valve (FESTO, Berkheim, Germany) was operated with nitrogen gas for pushing the melt to the nozzle. The PCL pellets were heated in a glass syringe (3 mL FORTUNA OPTIMA Luer Lock Tip, Poulten & Graf GmbH, Wertheim, Germany) with an electrical heating element connected to a proportional integral derivative (PID) controller (cTRON, JMMO, Metz Cedex, France). A metal flat-tipped nozzle (25G, Unimed Switzerland) was heated separately from the glass syringe and connected to a high voltage source (HCP 14–20000 Power supply, FuG Electronic GmbH, Schechen, Germany).

MEW Fiber Collection: Fibers were direct-written onto uncoated microscope slides (ECN 631–1552, VWR international GmbH, Germany). In first step, a wall of sequentially layered PCL fibers was printed with 20 layers to reach a height of ≈265 µm (set temperature = 90 °C, applied voltage = 6.0 kV, feeding pressure = 2.0 bar, collector velocity = 900 mm min^{-1}, collector distance = 3 mm). In second step, a crossing fiber was deposited over this wall, while the collector velocity (200–1200 mm min^{-1}), amplitude (20–1000 µm), and wavelength (100–3200 µm) were varied. To assess the influence of these crossing fibers on the shear properties of composites, MEW structures were printed in a radial manner to accommodate the loading direction of the rheometer. Afterwards, they were embedded into the different hydrogels. A variety of stabilizing architectures was tested. The control samples include a hydrogel only and one with walls only and no crossing fibers.

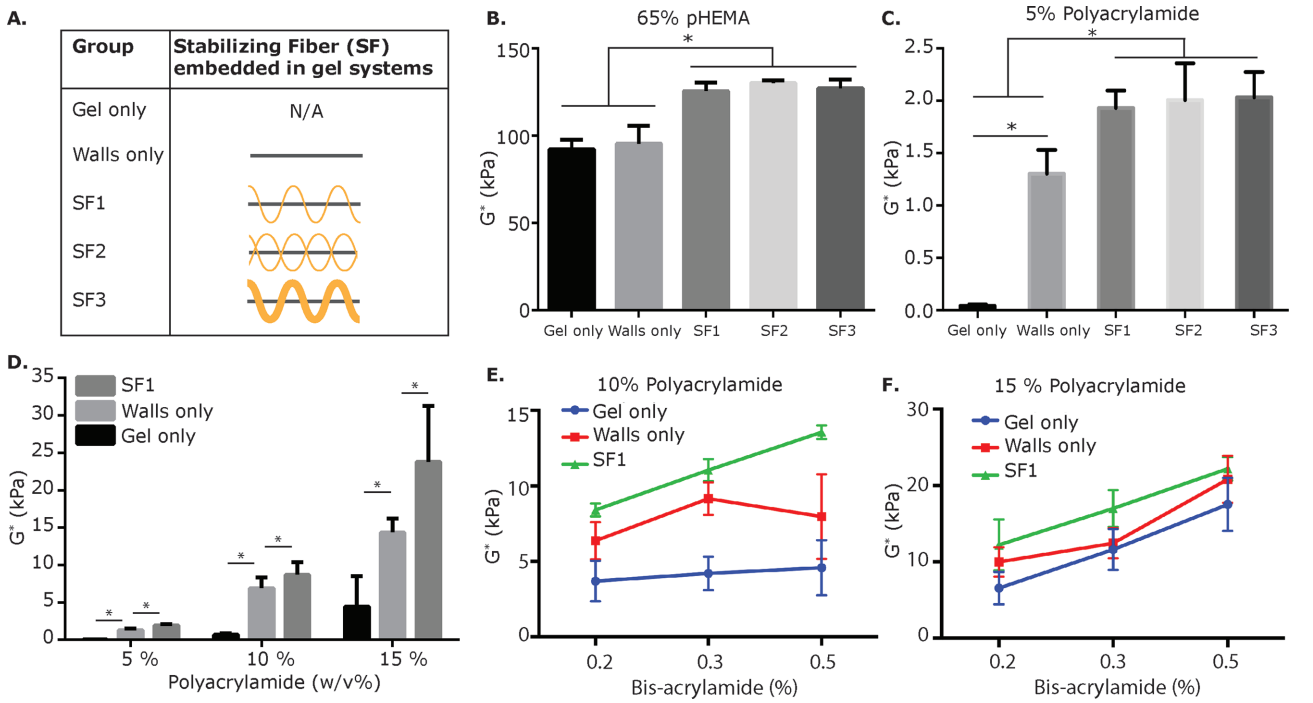

Figure 3. Effect of stabilizing fibers within fiber/hydrogel composites. A) Nomenclature of the stabilizing fiber structures when embedded within a hydrogel. B) Different designs of stabilizing fibers in pHEMA. C) Different designs of stabilizing fibers in the softer 5% polyacrylamide. D) Effect of stabilizing fibers (SF1) in 5%, 10%, and 15% polyacrylamide. E) Effect of stabilizing fibers in 10% polyacrylamide with 0.2%, 0.3%, and 0.5% bis-acrylamide representing an increase in hydrogel mesh size. F) Effect of stabilizing fibers in 15% polyacrylamide with 0.5%, 0.3%, and 0.2% bis-acrylamide. Data represented as mean ± SD, * = $p < 0.05$.

Visualization: Images were obtained using SEM (Zeiss CB 340, Carl Zeiss Microscopy GmbH, Göttingen, Germany), accelerating voltage = 2.0 kV. Prior to imaging, samples were coated with platinum (≈2 nm thick) (EM ACE600, Leica, Germany).

Embedding Samples in Hydrogel Composites: PCL scaffolds were embedded in 5%, 10%, and 15% polyacrylamide, as well as in pHEMA. For the polyacrylamide, a 30% acrylamide + bis-acrylamide solution (37.5:1 ratio, BIO-RAD) was diluted in phosphate-buffered-saline (PBS) and polymerized using 0.5% ammonium persulfate (APS, 10% w/v solution, Sigma-Aldrich) as initiator and 0.05% N,N,N′,N′-tertramethylethylenediamine (TEMED, Sigma-Aldrich) as a catalyst. To test the effect of the mesh size, acrylamide powder (BIO-RAD) and bis-acrylamide powder (Sigma-Aldrich) were diluted in PBS and polymerized with APS and TEMED. A solution of 65% 2-hydroxyethyl methacrylate (Sigma-Aldrich) and 35% deionized water was polymerized using 0.5% APS (Sigma-Aldrich) as an initiator and 0.5% TEMED a catalyst. All percentages are stated in wt% of the total volume. The hydrogel–fiber composites were all 26 mm in diameter and 1 mm in height.

Shear Testing: The complex shear modulus of the hydrogel composites ($n = 5$) was measured via oscillatory rheometry (plate–plate, diameter = 25 mm, gap = 1 mm) (Physica MCR301, Anton Paar GmbH, Baden-Wurttemberg, Germany). A frequency sweep was performed (0.05–500 rad s^{-1}, 0.01% strain) within the linear viscoelastic range, and the complex shear modulus at 10 rad s^{-1} was measured. Prior to testing, (physical) contact between plate and sample was ensured by applying a preload of 5% compression.

Statistics: An ANOVA, post hoc Bonferroni was used to test the difference between the groups. For the quantitative span measurements, $n = 3$ and 10 lines per sample were measured and $n = 5$ for the shear measurements. A difference was determined to be significant when $p < 0.05$, while data are presented as mean ± standard deviation.

Supporting Information

Supporting Information is available online from the Wiley Online Library or from the author.

Acknowledgements

This work was financially supported by the Dutch Arthritis Foundation (LLP-12); the European Community's Seventh Framework Programme (FP7/2007-2013) under grant agreement 309962 (HydroZONES). Further, the authors gratefully acknowledge the European Research Council under grant agreements 647426 (3D-JOINT) and 617989 (Design2Heal), as well as the German Research Foundation (DFG) State Major Instrumentation Programme for funding the Zeiss Crossbeam CB 340 scanning electron microscope (INST 105022/58-1 FUGG). The MEW device used for this study was built by G.H., while the support of the Hofvijverkring for P.D.D. is appreciated.

Conflict of Interest

The authors declare no conflict of interest.

Keywords

biofabrication, fiber reinforcement, hydrogels, mechanical properties, melt electrowriting

Received: August 11, 2017
Revised: October 5, 2017
Published online: December 14, 2017

[1] T. D. Brown, P. D. Dalton, D. W. Hutmacher, *Adv. Mater.* **2011**, *23*, 5651.
[2] P. D. Dalton, *Curr. Opin. Biomed. Eng.* **2017**, *2*, 49.
[3] P. D. Dalton, C. Vaquette, B. L. Farrugia, T. R. Dargaville, T. D. Brown, D. W. Hutmacher, *Biomater. Sci.* **2013**, *1*, 171.
[4] D. W. Hutmacher, T. Schantz, I. Zein, K. W. Ng, S. H. Teoh, K. C. Tan, *J. Biomed. Mater. Res.* **2001**, *55*, 203.
[5] J. N. H. Shepherd, S. T. Parker, R. F. Shepherd, M. U. Gillette, J. A. Lewis, R. G. Nuzzo, *Adv. Funct. Mater.* **2011**, *21*, 47.
[6] J. A. Lewis, *Adv. Funct. Mater.* **2006**, *16*, 2193.
[7] J. E. Smay, G. M. Gratson, R. F. Shepherd, J. Cesarano, J. A. Lewis, *Adv. Mater.* **2002**, *14*, 1279.
[8] T. D. Brown, A. Slotosch, L. Thibaudeau, A. Taubenberger, D. Loessner, C. Vaquette, P. D. Dalton, D. W. Hutmacher, *Biointerphases* **2012**, *7*, 13.
[9] G. Hochleitner, T. Jungst, T. D. Brown, K. Hahn, C. Moseke, F. Jakob, P. D. Dalton, J. Groll, *Biofabrication* **2015**, *7*, 035002.
[10] G. Hochleitner, A. Youssef, A. Hrynevich, J. N. Haigh, T. Jungst, P. D. Dalton, J. Groll, *BioNanoMaterials* **2016**, *17*, 159.
[11] T. D. Brown, P. D. Dalton, D. W. Hutmacher, *Prog. Polym. Sci.* **2016**, *56*, 116.
[12] W. C. M. Bognitzki, T. Frese, A. Schaper, M. Hellwig, M. Steinhart, A. Greiner, J. H. Wendorff, *Adv. Mater.* **2001**, *13*, 3.
[13] P. W. Gibson, H. L. Schreuder-Gibson, D. Rivin, *AIChE J.* **1999**, *45*, 5.
[14] D. H. Reneker, I. Chun, *Nanotechnology* **1996**, *7*, 216.
[15] M. L. Muerza-Cascante, D. Haylock, D. W. Hutmacher, P. D. Dalton, *Tissue Eng., Part B* **2015**, *21*, 187.
[16] J. Visser, F. P. W. Melchels, J. E. Jeon, E. M. van Bussel, L. S. Kimpton, H. M. Byrne, W. J. A. Dhert, P. D. Dalton, D. W. Hutmacher, J. Malda, *Nat. Commun.* **2015**, *6*, 6933.
[17] J. Malda, J. Visser, F. P. W. Melchels, T. Jungst, W. E. Hennink, W. J. A. Dhert, J. Groll, D. W. Hutmacher, *Adv. Mater.* **2013**, *25*, 5011.
[18] J. Coburn, M. Gibson, P. A. Bandalini, C. Laird, H. Q. Mao, L. Moroni, D. Seliktar, J. Elisseeff, *Smart Struct. Syst.* **2011**, *7*, 213.
[19] H. Prielipp, M. Knechtel, N. Claussen, S. K. Streiffer, H. Mullejans, M. Ruhle, J. Rodel, *Mater. Sci. Eng., A* **1995**, *197*, 19.
[20] S. R. Shin, H. Bae, J. M. Cha, J. Y. Mun, Y. C. Chen, H. Tekin, H. Shin, S. Farshchi, M. R. Dokmeci, S. Tang, A. Khademhosseini, *ACS Nano* **2012**, *6*, 362.
[21] D. Kai, M. P. Prabhakaran, B. Stahl, M. Eblenkamp, E. Wintermantel, S. Ramakrishna, *Nanotechnology* **2012**, *23*, 095705.
[22] W. Schuurman, V. Khristov, M. W. Pot, P. R. van Weeren, W. J. Dhert, J. Malda, *Biofabrication* **2011**, *3*, 021001.
[23] C. A. Engh, J. D. Bobyn, A. H. Glassman, *J. Bone Jt. Surg., Br. Vol.* **1987**, *69*, 45.
[24] F. Chen, G. Hochleitner, T. Woodfield, et al., *Biomacromolecules* **2016**, *17*, 208.
[25] G. Hochleitner, J. F. Hummer, R. Luxenhofer, et al., *Polymer* **2014**, *55*, 5017.
[26] S. Chiu-Webster, J. R. Lister, *J. Fluid Mech.* **2006**, *569*, 89.
[27] P. T. Brun, B. Audoly, N. M. Ribe, et al., *Phys. Rev. Lett.* **2015**, *114*, 174501.
[28] S. W. Morris, J. H. P. Dawes, N. M. Ribe, et al., *Phys. Rev. E* **2008**, *77*, 066218.
[29] T. Jungst, M. L. Muerza-Cascante, T. D. Brown, et al., *Polym. Int.* **2015**, *64*, 1086.
[30] C. E. Chang, V. H. Tran, J. B. Wang, et al., *Nano Lett.* **2010**, *10*, 726.
[31] S. W. Lee, H. J. Lee, J. H. Choi, et al., *Nano Lett.* **2010**, *10*, 347.
[32] M. A. Skylar-Scott, S. Gunasekaran, J. A. Lewis, *Proc. Natl. Acad. Sci. USA* **2016**, *113*, 6137.